HYBRID INTEGRAL TRANSFORM SOLUTION FOR MHD NATURAL CONVECTION IN CAVITIES

Jean Jorge Gomes da Silva, jeanjorge@ufpa.br
Emanuel Negrão Macêdo, enegrao@ufpa
João Nazareno Nonato Quaresma, quaresma@ufpa.br
Laboratory of Processes Simulation, School of Chemical Engineering, Institute of Technology, LSP/FEQ/ITEC
Universidade Federal do Pará, UFPA, Campus Universitário do Guamá, 66075-110, Belém, PA, Brazil

Renato Machado Cotta, cotta@mecanica.coppe.ufrj.br
Laboratory of Transmission and Technology of Heat-LTTC, Mechanical Engineering Department - POLI & COPPE
Universidade Federal do Rio de Janeiro, UFRJ, Cx. Postal 68503 – Cidade Universitária, 21945-970, Rio de Janeiro, RJ, Brazil

Abstract. MHD natural convection in laminar cavity flow of a Newtonian fluid is analyzed by making use of the streamfunction only formulation for the transient version of the Navier-Stokes and energy equations. The partial differential equations system describing the streamfunction and temperature distributions is then solved by the Generalized Integral Transform Technique (GITT). Numerical results are obtained for different Grashof and Hartmann numbers and Prandtl number equal to 0.71. Critical comparisons with previously reported numerical results are performed.

Keywords: Magnetohydrodynamics, Natural convection, Streamfunction formulation, Hybrid methods, Integral transforms.

1. INTRODUCTION

In recent years, a number of different approaches have been used for solving MHD flow in cavities in the primary purpose of validating these methods in the solution of coupled momentum and heat transport phenomena and electromagnetism, as governed by the continuity, Navier-Stokes, energy and Maxwell's equations, with the inherent complexity in light of their highly nonlinear and coupled characteristics. In order to assess the accuracy and effectiveness of such solution methodologies, the study of natural convection with or without a transverse magnetic field inside a square cavity has become a classical benchmark problem as in the works of De Vahl Davis (1983), Ramaswany *et al.* (1992), Sai *et al.* (1994), Barakos *et al.* (1994) and Colaço *et al.* (2009).

Oreper and Szekely (1983) were the first to propose a numerical solution to study the effect of a magnetic field on natural convection in square cavities, and have employed the finite difference method for obtaining the velocity and temperature distributions in terms of the streamfunction formulation in transient MHD flow. Al-Najem *et al.* (1998) also numerically studied laminar natural convection in a closed cavity with a transverse magnetic field. More recently, Colaço *et al.* (2009) used Radial Basis Functions (RBFs) to solve such system of coupled equations in steady state. The use of the Generalized Integral Transform Technique (GITT) to solve natural convection in laminar cavity flows has been advanced, for instance, by Leal and Cotta (1998), Leal *et al.* (1999) and Leal *et al.* (2000), providing a hybrid numerical-analytical solution for the velocity and temperature fields, working with a streamfunction only formulation for automatic satisfaction of the continuity equation and elimination of the pressure field.

The present paper is first of all aimed at advancing the hybrid integral transforms approach into handling natural convection problems under the action of a magnetic field. It also takes advantage of the developed hybrid solution to examine the influence of the magnetic field in the momentum and heat transfer in transient MHD flow in a square cavity, for conditions of moderate and high Grashof numbers. Following the previous works on natural convection with the GITT approach, the present analysis considers a formulation in terms of streamfunction only, which involves two independent variables, streamfunction and temperature. After a double integral transformation to eliminate the two space coordinates from the transformed system, the resulting nonlinear ordinary differential system in the time variable is numerically solved for the transformed potentials. Numerical results are then computed for different values of the governing parameters (Grashof, Hartmann and Prandtl numbers) and critical comparisons with previously reported results are performed to illustrate the adequacy of the present hybrid analytical-numerical solution methodology.

2. MATHEMATICAL FORMULATION

We consider a two-dimensional laminar flow in a square cavity, as illustrated in Figure 1. The cavity has an infinite extend along the z-axis, the lower and upper walls are insulated, while the side walls are maintained at different and constant temperatures, namely, the hot (T_h) and cold walls (T_c), respectively. The flow is in transient state and the fluid is Newtonian and electrically conductive. Also, the fluid properties are considered constant throughout the range of temperatures in the specific example. The temperature difference causes the movement through the onset of the buoyancy force. This term in the momentum equations is modeled using the Boussinesq approximation (density variation in the body force term only), as in (Gray and Giorgini, 1976). The fluid is permeated by a constant magnetic

field B_0 applied in the x-direction (from the left to the right wall), which creates a force opposing the buoyancy effect, the Lorentz force, represented by the vector product between the electrical current density and the magnetic field. Therefore, the equations governing the problem are the continuity, Navier-Stokes and energy equations, as well as the equation of electric charges conservation, Ohm's Law and Ampere-Maxwell's law in a moving medium, which are given by:
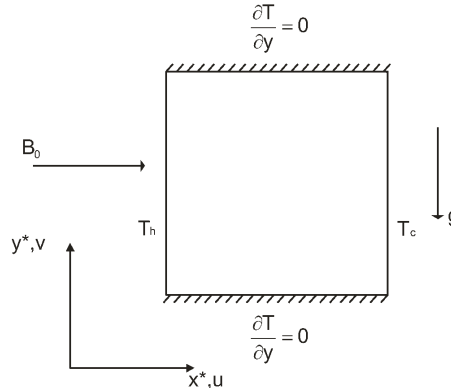
Figure 1. Geometric configuration of the natural convection problem with a transverse magnetic field.

$$\nabla . \boldsymbol{V}^* = 0 \tag{1.a}$$

$$\frac{\partial \boldsymbol{V}^*}{\partial t^*} + (\boldsymbol{V}^* . \nabla)\boldsymbol{V}^* = -\frac{1}{\rho}\nabla P + v\nabla^2\boldsymbol{V}^* - \beta_T g(T^* - T_0) + \frac{\boldsymbol{J}}{\rho}\times\boldsymbol{B} \tag{1.b}$$

$$\frac{\partial T^*}{\partial t^*} + (\boldsymbol{V}^* . \nabla)T^* = \alpha_T\nabla^2 T^* + \frac{\boldsymbol{J}}{\rho C_p}.(-\nabla E + \boldsymbol{V}^*\times\boldsymbol{B}) \tag{1.c}$$

$$\nabla . \boldsymbol{J} = 0 ; \quad \boldsymbol{J} = \sigma(-\nabla E + \boldsymbol{V}\times\boldsymbol{B}) ; \quad (\nabla\times\frac{\boldsymbol{B}}{\mu_0}) = \boldsymbol{J} \tag{1.d-f}$$

where, v is the kinematic viscosity, β_T is the coefficient of thermal expansion, σ is the electrical conductivity and μ_0 is the magnetic permeability of the vacuum. In this study the effects of polarization and magnetization were neglected. The magnetic Reynolds number is considered to be very small. Also, the effects of Joule heating and viscous dissipation are assumed to be very small, thus we can neglect the second term on the right hand side of Eq. (1.c).

In Eq. (1.e), the Ohm's Law, E is the electric potential and $-\nabla E$ the electric field associated to this potential. It can be shown that that the electric field vanishes everywhere for the situation of electrically insulating boundaries (Garandet *et al.*, 1992). Also, it is easy to show by substituting Eq. (1.f) into Eq. (1.d), that for a two-dimensional flow, the equation of conservation of charge is automatically satisfied.

Now, we recall the usual definition of the streamfunction, in the form:

$$u^* = \frac{\partial \psi^*}{\partial y^*} ; \qquad v^* = -\frac{\partial \psi^*}{\partial x^*} \tag{2.a,b}$$

and the following dimensionless quantities:

$$x = \frac{x^*}{L} ; \quad y = \frac{y^*}{L} ; \quad \psi = \frac{\psi^*}{\alpha_T} ; \quad t = \frac{\alpha_T t^*}{L^2} ; \quad T = \frac{T^* - T_c}{T_h - T_c} \tag{3.a-e}$$

where the subscript "*" identifies the dimensional variables, and L is the length of the cavity.

Substituting Eqs. (2.a,b) into Eqs. (1.a-c), we obtain the vorticity transport and energy equations in terms of the streamfunction and temperature only, which in dimensionless form is given by:

$$\frac{\partial}{\partial t}(\nabla^2\psi) = \frac{\partial(\psi, \nabla^2\psi)}{\partial(x, y)} + Pr \nabla^4\psi - Pr Ha^2 \frac{\partial^2\psi}{\partial x^2} - Ra Pr \frac{\partial T}{\partial x} \tag{4}$$

$$\frac{\partial T}{\partial t} = \frac{\partial(\psi, T)}{\partial(x, y)} + \nabla^2 T \tag{5}$$

Here, the notation $\partial(a,b)/\partial(c,d)$ is similar to the Jacobian determinant, and *Ha*, *Ra*, *Pr* and *Gr* are the Hartmann, Rayleigh, Prandtl and Grashof numbers, respectively, which are defined as:

$$Ha = B_0 L \sqrt{\frac{\sigma}{\mu_0}}; \quad Ra = \frac{g\beta_T(T_h - T_c)L^3}{\alpha_T \nu}; \quad Pr = \frac{\nu}{\alpha_T}; \quad Gr = \frac{g\beta_T(T_h - T_c)L^3}{\nu^2} = \frac{Ra}{Pr} \tag{6.a-d}$$

The initial and boundary conditions, in dimensionless form, needed to complete the mathematical formulation, are:

$$T(x,y,0) = \psi(x,y,0) = 0 \quad \text{for} \quad t = 0 \tag{7.a,b}$$

$$\psi = \frac{\partial \psi}{\partial x} = 0; \quad T = 1 \text{ at } x = 0; \quad \psi = \frac{\partial \psi}{\partial x} = T = 0 \text{ at } x = 1 \tag{7.c-h}$$

$$\psi = \frac{\partial \psi}{\partial y} = \frac{\partial T}{\partial y} = 0 \text{ at } y = 0; \quad \psi = \frac{\partial \psi}{\partial y} = \frac{\partial T}{\partial y} = 0 \text{ at } y = 1 \tag{7.i-o}$$

3. SOLUTION METHODOLOGY

The first step in the solution procedure is the filtering strategy to enhance convergence of the eigenfunction expansions, by making the boundary conditions homogeneous. The simplest choice of a filtering solution for the temperature field is extracted from the steady pure conduction problem, and the filter is written as:

$$T(x,y,t) = \theta(x,y,t) + T_F(x); \quad T_F(x) = 1 - x \tag{8.a,b}$$

A filter based on the transient version of the conduction problem can be obtained, but for purposes of homogenization of boundary conditions of the temperature field, it suffices to take Eq. (8.b) as a simple filter. Now, substituting Eqs. (8) into the original problem, Eqs. (4), (5) and (7), we obtain:

$$\frac{\partial}{\partial t}(\nabla^2 \psi) = \frac{\partial(\psi, \nabla^2 \psi)}{\partial(x,y)} + Pr\nabla^4\psi - Pr\,Ha^2 \frac{\partial^2 \psi}{\partial x^2} - Ra\,Pr\frac{\partial \theta}{\partial x} + Ra\,Pr \tag{9}$$

$$\frac{\partial \theta}{\partial t} = \frac{\partial(\psi, \theta)}{\partial(x,y)} + \frac{\partial \psi}{\partial y} + \nabla^2\theta \tag{10}$$

$$\psi(x,y,0) = 0, \quad \theta(x,y,0) = x - 1; \quad 0 \le x \le 1, \; 0 \le y \le 1 \tag{11.a,b}$$

$$\psi = \frac{\partial \psi}{\partial x} = \theta = 0 \text{ at } x = 0; \quad \psi = \frac{\partial \psi}{\partial x} = \theta = 0 \text{ at } x = 1 \tag{11.c-h}$$

$$\psi = \frac{\partial \psi}{\partial y} = \frac{\partial \theta}{\partial y} = 0 \text{ at } y = 0; \quad \psi = \frac{\partial \psi}{\partial y} = \frac{\partial \theta}{\partial y} = 0 \text{ at } y = 1 \tag{11.i-o}$$

The next step is the selection of the eigenfunction basis in each direction, x and y, for each individual potential, ψ and θ. Following previous developments (Pérez Guerrero, 1995; Leal, 1996), for the streamfunction expansion, it is proposed to use fourth-order eigenvalue problems basic to the integral transform solution of the biharmonic equation (Cotta, 1993) as:

- x-direction:

$$\frac{d^4 X_i(x)}{dx^4} = \alpha_i^4 X_i(x), \quad 0 < x < 1 \tag{12.a}$$

$$X_i(0) = 0; \quad \frac{dX_i(0)}{dx} = 0; \quad X_i(1) = 0; \quad \frac{dX_i(1)}{dx} = 0 \tag{12.b-e}$$

with the solution for the eigenfunctions $X_i(x)$ and the transcendental equation for computing the eigenvalues, given by:

$$X_i(x) = \begin{cases} \dfrac{cos[\alpha_i(x - 1/2)]}{cos(\alpha_i/2)} - \dfrac{cosh[\alpha_i(x - 1/2)]}{cosh(\alpha_i/2)}, & \text{for } i = 1,3,5,... \\ \dfrac{sin[\alpha_i(x - 1/2)]}{sin(\alpha_i/2)} - \dfrac{sinh[\alpha_i(x - 1/2)]}{sinh(\alpha_i/2)}, & \text{for } i = 2,4,6,... \end{cases} \tag{12.f,g}$$

$$tanh(\alpha_i/2) = \begin{cases} -tan(\alpha_i/2), & \text{for } i = 1,3,5,... \\ tan(\alpha_i/2), & \text{for } i = 2,4,6,... \end{cases} \tag{12.h,i}$$

satisfying the following orthogonality property:

$$\int_0^1 X_i(x)X_j(x)dx = \begin{cases} 0, & i \neq j \\ Mx_i, & i = j \end{cases} \tag{12.j,k}$$

The norm or normalization integral Mx_i is obtained from

$$Mx_i = \int_0^1 X_i^2(x)dx = 1 \tag{12.l}$$

The normalized eigenfunctions $\tilde{X}_i(x)$ are then defined by:

$$\tilde{X}_i(x) = \frac{X_i(x)}{Mx_i^{1/2}} \tag{12.m}$$

which in this case coincide with the original eigenfunctions themselves. Similarly, for the y direction, we propose a fourth order eigenvalue problem:

- y-direction:

$$\frac{d^4 Y_\ell(y)}{dy^4} = \beta_\ell^4 Y_\ell(y), \quad 0 < y < 1 \tag{13.a}$$

$$Y_\ell(0) = 0; \quad \frac{dY_\ell(0)}{dy} = 0; \quad Y_\ell(1) = 0; \quad \frac{dY_\ell(1)}{dy} = 0 \tag{13.b-e}$$

Similarly to the x-direction, Eqs. (13.a) to (13.e) are analytically solved to yield the eigenfunctions, transcendental equation for computing the eigenvalues, orthogonality property, normalization integral, and normalized eigenfunctions, respectively, as:

$$Y_\ell(y) = \begin{cases} \dfrac{cos[\beta_\ell(y-1/2)]}{cos(\beta_\ell/2)} - \dfrac{cosh[\beta_\ell(y-1/2)]}{cosh(\beta_\ell/2)}, & \text{for} \quad \ell = 1,3,5,... \\[3mm] \dfrac{sin[\beta_\ell(y-1/2)]}{sin(\beta_\ell/2)} - \dfrac{sinh[\beta_\ell(y-1/2)]}{sinh(\beta_\ell/2)}, & \text{for} \quad \ell = 2,4,6,... \end{cases} ; \quad tanh(\beta_\ell/2) = \begin{cases} -tan(\beta_\ell/2), & \text{for} \quad \ell = 1,3,5,... \\ tan(\beta_\ell/2), & \text{for} \quad \ell = 2,4,6,... \end{cases} \tag{13.f-i}$$

$$\int_0^1 Y_\ell(y)Y_m(y)dy = \begin{cases} 0, & \ell \neq m \\ My_\ell, & \ell = m \end{cases}; \quad My_\ell = \int_0^1 Y_\ell^2(y)dy = 1; \quad \tilde{Y}_\ell(y) = \frac{Y_\ell(y)}{My_\ell^{1/2}} \tag{13.j-m}$$

For the temperature expansion, the following second order eigenvalue problems are proposed, as follows:

- x-direction:

$$\frac{d^2 \phi_i(x)}{dx^2} + \lambda_i^2 \phi_i(x) = 0, \quad 0 < x < 1 \tag{14.a}$$

$$\phi_i(0) = 0; \quad \phi_i(1) = 0 \tag{14.b,c}$$

Equations (14.a) to (14.c) are analytically solved, to yield

$$\phi_i(x) = sin(\lambda_i x); \quad \lambda_i = i\pi, \quad \text{for} \quad i = 1,2,3,... \tag{14.d,e}$$

$$\int_0^1 \phi_i(x)\phi_j(x)dx = \begin{cases} 0, & i \neq j \\ Nx_i, & i = j \end{cases}; \quad Nx_i = \int_0^1 \phi_i^2(x)dx = 1/2; \quad \tilde{\phi}_i(x) = \frac{\phi_i(x)}{Nx_i^{1/2}} \tag{14.f-i}$$

- y-direction:

$$\frac{d^2 \Gamma_\ell(y)}{dy^2} + \mu_\ell^2 \Gamma_\ell(y) = 0, \quad 0 < y < 1 \tag{15.a}$$

$$\frac{d\Gamma_\ell(0)}{dy} = 0; \quad \frac{d\Gamma_\ell(1)}{dy} = 0 \tag{15.b,c}$$

Similarly, Eqs. (15.a) to (15.c) are analytically solved, to yield:

$$\Gamma_\ell(y) = cos(\mu_\ell y); \quad \mu_\ell = (\ell - 1)\pi, \quad for \quad \ell = 1,2,3,... \tag{15.d,e}$$

$$\int_0^1 \Gamma_\ell(y)\Gamma_m(y)dy = \begin{cases} 0, & \ell \neq m \\ Ny_\ell, & \ell = m \end{cases}; \quad Ny_\ell = \int_0^1 \Gamma_\ell(y)dy = \begin{cases} 1, & \ell = 1 \\ 1/2, & \ell > 1 \end{cases}; \quad \tilde{\Gamma}_\ell(y) = \frac{\Gamma_\ell(y)}{Ny_\ell^{1/2}} \tag{15.f-j}$$

The eigenvalue problems above allow the determination of the following integral transform pairs for the streamfunction and temperature fields, respectively:

$$\bar{\tilde{\psi}}_{i\ell}(t) = \int_0^1 \int_0^1 \tilde{X}_i(x)\tilde{Y}_\ell(y)\psi(x, y, t)dydx, \quad transform; \quad \psi(x, y, t) = \sum_{i=1}^\infty \sum_{\ell=1}^\infty \tilde{X}_i(x)\tilde{Y}_\ell(y)\bar{\tilde{\psi}}_{i\ell}(t), \quad inverse \tag{16.a,b}$$

$$\bar{\tilde{\theta}}_{i\ell}(t) = \int_0^1 \int_0^1 \tilde{\phi}_i(x)\tilde{\Gamma}_\ell(y)\theta(x, y, t)dydx, \quad transform; \quad \theta(x, y, t) = \sum_{i=1}^\infty \sum_{\ell=1}^\infty \tilde{\phi}_i(x)\tilde{\Gamma}_\ell(y)\bar{\tilde{\theta}}_{i\ell}(t), \quad inverse \tag{17.a,b}$$

Applying the double integral transformations given by Eqs. (16.a) and (17.a), into the streamfunction and temperature problems, respectively, it results in the following infinite coupled transformed ODE system:

$$\sum_{j=1}^\infty \sum_{m=1}^\infty A_{ij\ell m} \frac{d\bar{\tilde{\psi}}_{jm}}{dt} = Pr(\alpha_i^4 + \beta_\ell^4)\bar{\tilde{\psi}}_{jm} + \sum_{j=1}^\infty \sum_{m=1}^\infty \left[2Pr B_{ij\ell m} + \sum_{k=1}^\infty \sum_{n=1}^\infty \left(C_{ijk\ell mn} - D_{ijk\ell mn} \right)\bar{\tilde{\psi}}_{kn} - Pr Ha^2 E_{ij\ell m} \right]\bar{\tilde{\psi}}_{jm} - $$
$$PrRa\left[\sum_{j=1}^\infty \sum_{m=1}^\infty F_{ij\ell m}\bar{\tilde{\phi}}_{jm} - G_{i\ell} \right] \tag{18.a}$$

$$\frac{d\bar{\tilde{\theta}}_{i\ell}}{dt} = -(\lambda_i^2 + \mu_\ell^2)\bar{\tilde{\theta}}_{i\ell} + \sum_{j=1}^\infty \sum_{m=1}^\infty \left[\sum_{k=1}^\infty \sum_{n=1}^\infty \left(H_{ijk\ell mn} - I_{ijk\ell mn} \right)\bar{\tilde{\theta}}_{kn} + J_{ij\ell m} \right]\bar{\tilde{\psi}}_{jm} \tag{18.b}$$

The same integral transformation is operated on the initial conditions, providing:

$$\bar{\tilde{\psi}}_{i\ell}(0) = 0; \qquad \bar{\tilde{\theta}}_{i\ell}(0) = \bar{\tilde{f}}_{i\ell} \tag{18.c,d}$$

The above coefficients are computed from the following definite integrals:

$$A_{ij\ell m} = \left(\int_0^1 \tilde{X}_i \frac{d^2 \tilde{X}_j}{dx^2} dx \right)\delta_{\ell m} + \left(\int_0^1 \tilde{Y}_\ell \frac{d^2 \tilde{Y}_m}{dy^2} dy \right)\delta_{ij}; \qquad B_{ij\ell m} = \left(\int_0^1 \tilde{X}_i \frac{d^2 \tilde{X}_j}{dx^2} dx \right)\left(\int_0^1 \tilde{Y}_\ell \frac{d^2 \tilde{Y}_m}{dy^2} dy \right) \tag{19.a,b}$$

$$C_{ijk\ell mn} = \left(\int_0^1 \tilde{X}_i \frac{d\tilde{X}_j}{dx} \frac{d^2 \tilde{X}_k}{dx^2} dx \right)\left(\int_0^1 \tilde{Y}_\ell \tilde{Y}_m \frac{d\tilde{Y}_n}{dy} dy \right) + \left(\int_0^1 \tilde{X}_i \frac{d\tilde{X}_j}{dx} \tilde{X}_k dx \right)\left(\int_0^1 \tilde{Y}_\ell \tilde{Y}_m \frac{d^3 \tilde{Y}_n}{dy^3} dy \right) \tag{19.c}$$

$$D_{ijk\ell mn} = \left(\int_0^1 \tilde{X}_i \tilde{X}_j \frac{d^3 \tilde{X}_k}{dx^3} dx \right)\left(\int_0^1 \tilde{Y}_\ell \frac{d\tilde{Y}_m}{dy}\tilde{Y}_n dy \right) + \left(\int_0^1 \tilde{X}_i \tilde{X}_j \frac{d\tilde{X}_k}{dx} dx \right)\left(\int_0^1 \tilde{Y}_\ell \frac{d\tilde{Y}_m}{dy} \frac{d^3 \tilde{Y}_n}{dy^3} dy \right) \tag{19.d}$$

$$E_{ij\ell m} = \left(\int_0^1 \tilde{X}_i \frac{d^2 \tilde{X}_j}{dx^2} dx \right)\delta_{\ell m}; \quad F_{ij\ell m} = \left(\int_0^1 \tilde{X}_i \tilde{\phi}_j dx \right)\left(\int_0^1 \tilde{Y}_\ell \tilde{\Gamma}_m dy \right); \qquad G_{i\ell} = \left(\int_0^1 \tilde{X}_i dx \right)\left(\int_0^1 \tilde{Y}_\ell dy \right) \tag{19.e-g}$$

$$H_{ijk\ell mn} = \left(\int_0^1 \tilde{\phi}_i \frac{d\tilde{X}_j}{dx} \tilde{\phi}_k dx \right)\left(\int_0^1 \tilde{\Gamma}_\ell \tilde{Y}_m \frac{d\tilde{\Gamma}_n}{dy} dy \right); \qquad I_{ijk\ell mn} = \left(\int_0^1 \tilde{\phi}_i \tilde{X}_j \frac{d\tilde{\phi}_k}{dx} dx \right)\left(\int_0^1 \tilde{\Gamma}_\ell \frac{d\tilde{Y}_m}{dy} \tilde{\Gamma}_n dy \right) \tag{19.h,i}$$

$$J_{ij\ell m} = \left(\int_0^1 \tilde{\phi}_i \tilde{X}_j dx \right)\left(\int_0^1 \tilde{\Gamma}_\ell \frac{d\tilde{Y}_m}{dy} dy \right); \quad \bar{\tilde{f}}_{i\ell} = \left[\int_0^1 (x - 1)\tilde{\phi}_i dx \right]\left(\int_0^1 \tilde{\Gamma}_\ell dy \right); \quad \delta_{ij} = \begin{cases} 0, & i \neq j \\ 1, & i = j \end{cases}; \quad \delta_{\ell m} = \begin{cases} 0, & \ell \neq m \\ 1, & \ell = m \end{cases} \tag{19.j-m}$$

The coefficients above are analytically obtained through symbolic manipulation packages (Wolfram, 2005). Equations (18) form an infinite system of first order nonlinear coupled ODEs. For computational purposes the system must be truncated to a sufficiently large finite order so as to achieve converged solutions for a given desired accuracy.

Before defining a truncated version of the initial value problem to be numerically solved, system (18) is rewritten so as to account for the most important contributions in an orderly manner, thus transforming the nested double summations into single ones, reordered from the expected largest to the smallest transformed potentials. A fairly simple reordering scheme for multidimensional eigenfunction expansions is described in greater detail in Mikhailov and Cotta (1996) and Cotta and Mikhailov (1997), aimed at saving computational effort while providing convergence of the expansions with the minimum number of equations in the transformed system. Here, the same criterion was selected and the reordering procedure involves the summation of the squared eigenvalues in each direction, in the form:

$$\alpha_i^4 + \beta_\ell^4 = \alpha_p^4; \qquad \lambda_i^2 + \mu_\ell^2 = \lambda_p^2 \tag{20.a,b}$$

Then, the indices related to the streamfunction and temperature expansions are reorganized into a single index, as:

$$\sum_{i=1}^{\infty}\sum_{\ell=1}^{\infty}\rightarrow\sum_{p=1}^{\infty}; \qquad \sum_{j=1}^{\infty}\sum_{m=1}^{\infty}\rightarrow\sum_{q=1}^{\infty}; \qquad \sum_{k=1}^{\infty}\sum_{n=1}^{\infty}\rightarrow\sum_{r=1}^{\infty} \qquad (21.\text{a-c})$$

System (18) is then rewritten as:

$$\sum_{q=1}^{\infty}A_{pq}\frac{d\bar{\psi}_q}{dt} = Pr\,\alpha_p^4\bar{\psi}_p + \sum_{q=1}^{\infty}\left[2Pr\,B_{pq} + \sum_{r=1}^{\infty}\left(C_{pqr}-D_{pqr}\right)\bar{\psi}_r - Pr\,Ha^2E_{pq}\right]\bar{\psi}_q - PrRa\left[\sum_{q=1}^{\infty}F_{pq}\bar{\phi}_q - G_p\right] \qquad (22.\text{a})$$

$$\frac{d\bar{\theta}_p}{dt} = -\lambda_p^2\bar{\theta}_p + \sum_{q=1}^{\infty}\left[\sum_{r=1}^{\infty}\left(H_{pqr}-I_{pqr}\right)\bar{\theta}_r + J_{pq}\right]\bar{\psi}_q \qquad (22.\text{b})$$

$$\bar{\psi}_p(0) = 0; \qquad \bar{\theta}_p(0) = \bar{f}_p \qquad (22.\text{c,d})$$

System (22) is now in the appropriate format for numerical solution through dedicated routines for stiff initial value problems, such as the subroutine DIVPAG from the IMSL Library (1991), which is well tested and capable of handling such situations, offering an automatic accuracy control scheme. For computational purposes, the expansions are then truncated to *NV* and *NT* terms for the streamfunction and temperature fields, respectively, where the truncation orders are selected so as to reach the user requested accuracy target in the final solution. This subroutine solves initial value problems of the form:

$$A\boldsymbol{y}' = f(\boldsymbol{y},t); \qquad \boldsymbol{y}(0) = \boldsymbol{y}_0 \qquad (23.\text{a,b})$$

where, in this notation, the solution vector composed of *NV+NT* ODEs is given by:

$$\boldsymbol{y} = \left\{\bar{\psi}_1(t),...,\bar{\psi}_{NV}(t),\bar{\theta}_1(t),...,\bar{\theta}_{NT}(t)\right\}^T \qquad (24)$$

From the solution of system (22) above for the transformed potentials, the streamfunction and the temperature fields are then readily obtained from the inversion formulae (16.b) and (17.b), as well as other quantities of practical interest, such as the horizontal and vertical velocity components, in the form:

$$u = \sum_{i=1}^{\infty}\sum_{\ell=1}^{\infty}\tilde{X}_i(x)\frac{d\tilde{Y}_\ell(y)}{dy}\bar{\tilde{\psi}}_{i\ell}(t); \qquad v = -\sum_{i=1}^{\infty}\sum_{\ell=1}^{\infty}\frac{d\tilde{X}_i(x)}{dx}\tilde{Y}_\ell(y)\bar{\tilde{\psi}}_{i\ell}(t) \qquad (25.\text{a,b})$$

From the definitions for the maximum (or minimum) local (at the hot wall x = 0), average (at any "x" cross-section) and global (across the cavity) Nusselt numbers, we obtain:

$$Nu_M = -\frac{\partial T}{\partial x}\bigg|_{x=0}; \quad Nu_x = \int_0^1\left[u(x,y,t)T(x,y,t) - \frac{\partial T(x,y,t)}{\partial x}\right]dy; \quad \bar{Nu} = \int_0^1 Nu_x dx \qquad (26.\text{a-c})$$

The numerical values of Nusselt numbers defined in Eqs. (26) are computed from the substitution of the inversion formulae (16.b) and (17.b) into such expressions.

4. RESULTS AND DISCUSSION

A Fortran 95/2003 code was built and implemented on a PC-PENTIUM Dual Core 2.80 GHz. Test cases were analyzed for Grashof numbers equal to 10^4 and 10^6, Hartmann number in the range from 0<Ha<100, while the Prandtl number was taken equal to 0.71 in all cases. The subroutine DIVPAG of the IMSL Library (1991) was employed for the transformed system solution, always with a relative error target of 10^{-10}. The coefficients were analytically evaluated with the symbolic manipulation package *Mathematica* (Wolfram, 2005). Results are presented and compared for different times of interest during the transient process, in terms of the dimensionless velocity components, dimensionless temperature, local and average Nusselt numbers. Also, some steady state results have been compared with results available in the literature.

Figure 2 shows the behavior of the streamfunction isolines at four selected times for Gr = 10^4 and Ha = 0 and 50. It is observed that for the shortest time, t = 0.005, there is the formation of a distinct boundary layer in the flow along the hot wall, besides there is the presence of a clockwise distorted vortex near the same wall. The vortex moves over time to the geometric center of the cavity to assume a rounded configuration at tsteady state, here illustrated by the curves for t = 0.93. The presence of a transverse magnetic field in the square cavity (Ha = 50) makes the rounded and central vortex at the geometric center of the cavity undergo a vertical stretch. This behavior is observed in the streamfunction isolines for various times, which shows that over time arises a tendency to break up the central vortex towards the appearance of secondary vortices.

Temperature isolines are shown in Fig. 3 for Gr = 10^4, for a few selected time values, and make it clear that in the early stage of the process the temperature field evolves similarly to a pure conduction problem, characterized by higher temperature gradients in the vicinity of the hot wall. As time progresses, gradually reduces these gradients and the bulk temperature increases, while the contours acquire the typical aspect of the presence of convection. The isotherms for Ha = 50 show that, initially, the process continues with the aspect of a pure conduction problem, and as the process moves forward in time the gradients are kept fairly high along the horizontal direction, and this characteristic is maintained. The isotherms are almost parallel to the vertical walls, indicating that most of the heat transfer process is by conduction.
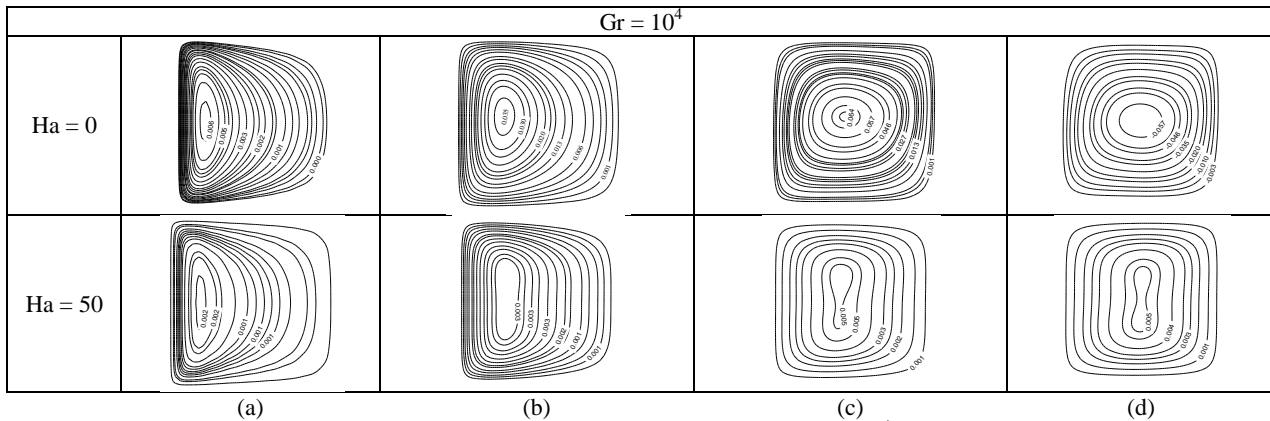
Figure 2. Streamfunction isolines for different times with Gr = 10^4 and Ha = 0 and 50.
(a) t = 0.005; (b) t = 0.02; (c) t = 0.1; (d) t = 0.93.
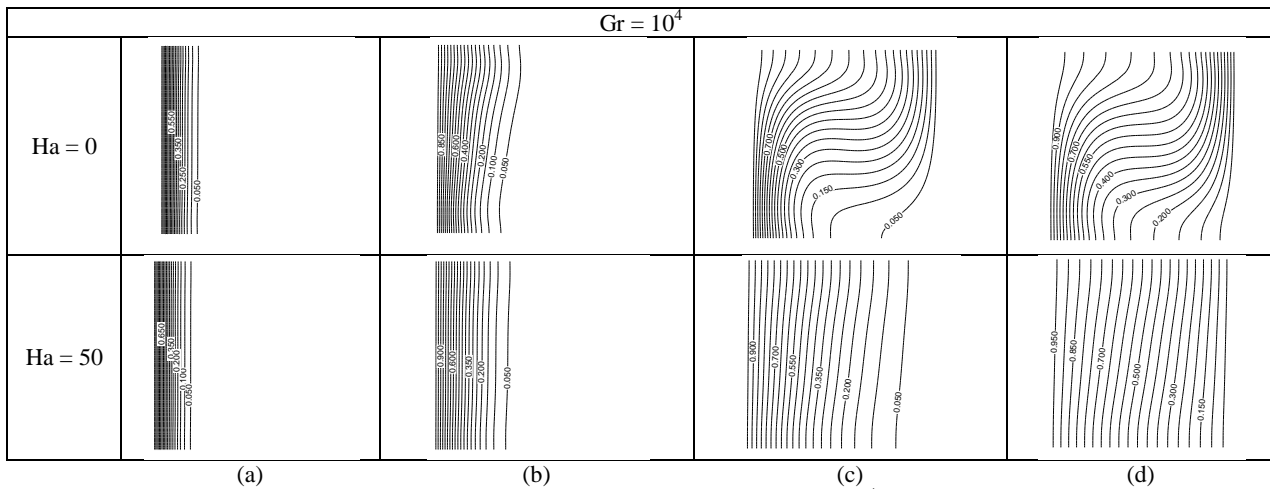
Figure 3. Temperature isolines for different times with Gr = 10^4 and Ha = 0 and 50.
(a) t = 0.005; (b) t = 0.02; (c) t = 0.1; (d) t = 0.93.

The second Grashof number examined is Gr = 10^6, which corresponds to conditions in which thermal effects are of greater magnitude, the convection evolves extremely quickly, and we observe the emergence of marked movements of internal waves. Thus, the magnetic field necessary to suppress the natural convection must be stronger than those previously discussed for Gr = 10^4. Therefore, this behavior is shown in Figure 4 for the streamfunction isolines with Gr = 10^6 and Ha = 0 and 100 at four different times. Now, with the presence of stronger magnetic field, Ha = 100, with the advancement of the transient process the axis of the central vortex is rotated in a counterclockwise direction, and this effect is due to the suppression of convection by the Lorentz force.

Figure 5 shows the isotherms for the cases Gr = 10^6 and Ha = 0 and 100 at four different times. Again, it is evident the formation of a distinct vertical boundary layer along the heated wall early in the process and the formation of at least two vortices at the geometric center of the cavity for the largest time, t = 0.93. The discharge of a jet by the heated side wall form an initially horizontal layer of intrusion that occurs along the upper horizontal wall of the cavity, as shown in Fig. 5.a for t = 0.005. With the advancement of the transient process, the horizontal flow invades the center of the cavity resulting in the formation of a thermally stratified core, where the temperature increases monotonically as a function of the coordinate y, and tend to be parallel to the vertical wall.

Gr = 10^6				
Ha = 0				
Ha = 100				
	(a)	(b)	(c)	(d)
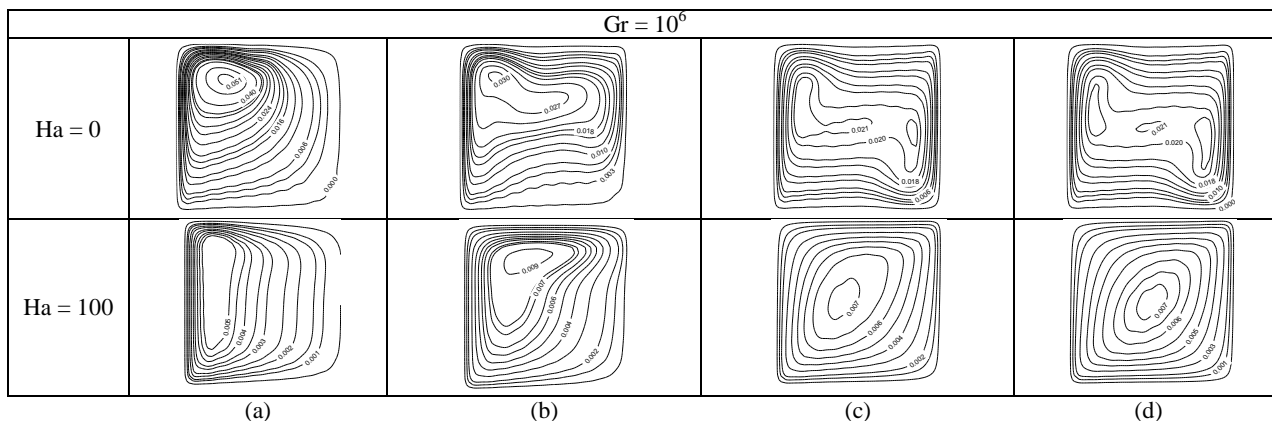
Figure 4. Streamfunction isolines for different times with Gr = 10^6 and Ha = 0 and 100.
(a) t = 0.005; (b) t = 0.02; (c) t = 0.1; (d) t = 0.93.

Gr = 10^6				
Ha = 0				
Ha = 100				
	(a)	(b)	(c)	(d)
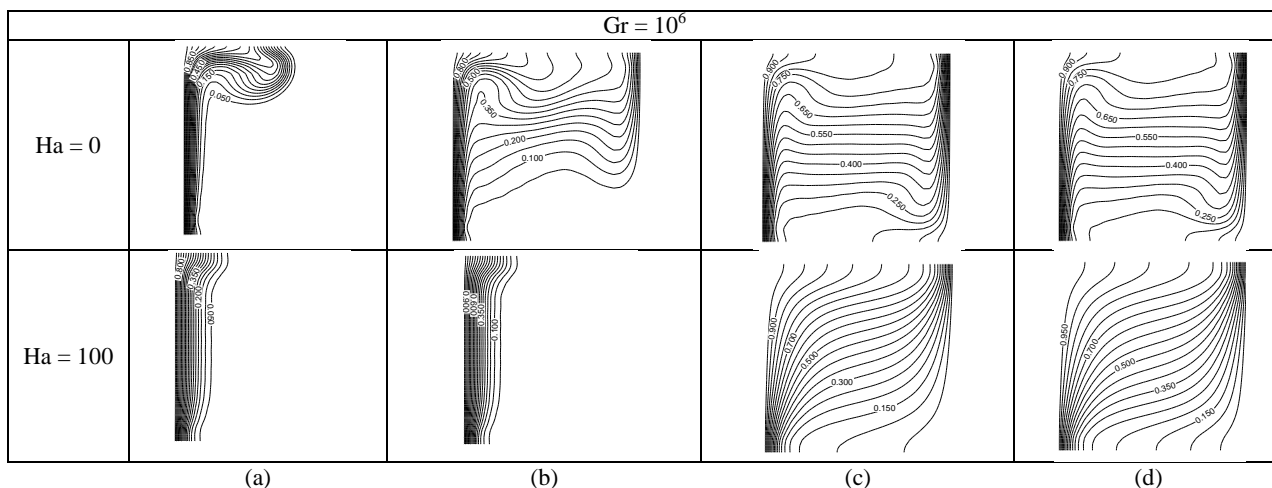
Figure 5. Temperature isolines for different times with Gr = 10^6 and Ha = 0 and 100.
(a) t = 0.005; (b) t = 0.02; (c) t = 0.1; (d) t = 0.93.

The agreement of the results for the global Nusselt number obtained with the GITT approach, with those of both Colaço *et al.* (2009) and Al-Najem *et al.* (1998), is quite reasonable, with a relative error as observed in Table 1, always below 5%, for Gr = 10^4 and all Hartmann numbers studied.

Table 1. Comparison of the present results for the global Nusselt number with previously reported solutions for Gr = 10^4 and Ha=0, 10, 25, and 50, in steady state.

Global Nusselt number					
Ha	Present	Colaço *et al.* (2009)	Error(%)	Al-Najem *et al.* (1998)	Error(%)
0	2.01	2.02	0.50	2.01	0.00
10	1.69	1.70	0.59	1.69	0.00
25	1.16	1.17	0.85	1.14	1.75
50	1.01	0.97	4.12	1.00	1.00

The behavior of the velocity field is more evident when we observe Figure 6.a, where it is compared the present results obtained by the GITT approach with those of Colaço *et al.* (2009) for the velocity profile in the x-direction in the vertical midplane of the cavity (x = 1/2), for Gr = 10^4 and steady state. For the lowest Hartmann number analyzed (Ha = 0), the behavior of the velocity field at this point indicates the existence of a vortex and a point of zero velocity (y = 1/2). The high gradients from the center to the vertical walls indicate the existence of convective currents. On the other hand, for the largest Hartmann number analyzed (Ha = 50), the behavior indicates that the magnetic field suppresses convective currents inside the cavity. Results for the temperature field obtained by the GITT are also compared with those of Colaço *et al.* (2009), in Figure 6.b in the median horizontal plane of the cavity (y = 1/2). Heat transfer by conduction takes place predominantly with high gradients at the largest Hartmann number. A decrease in these gradients is observed and a typical aspect of the presence of convection is observed for the lowest Hartmann

number. Also, Figs. 6.a and 6.b show the excellent agreement between the present results with those of Colaço *et al.* (2009).

Similar comparisons are provided in Figures 7.a and 7.b, for the velocity and temperature fields, respectively, for a higher Grashof number (Gr = 10^6). Again, an excellent agreement is verified between the two different approaches for this case. For lower Hartmann numbers (H = 0 and 15), despite showing the same trend, a slight deviation from the results obtained by Colaço et al. (2009) is evident. The differences for the temperature field are less evident, and an excellent agreement is verified for all Hartmann numbers.
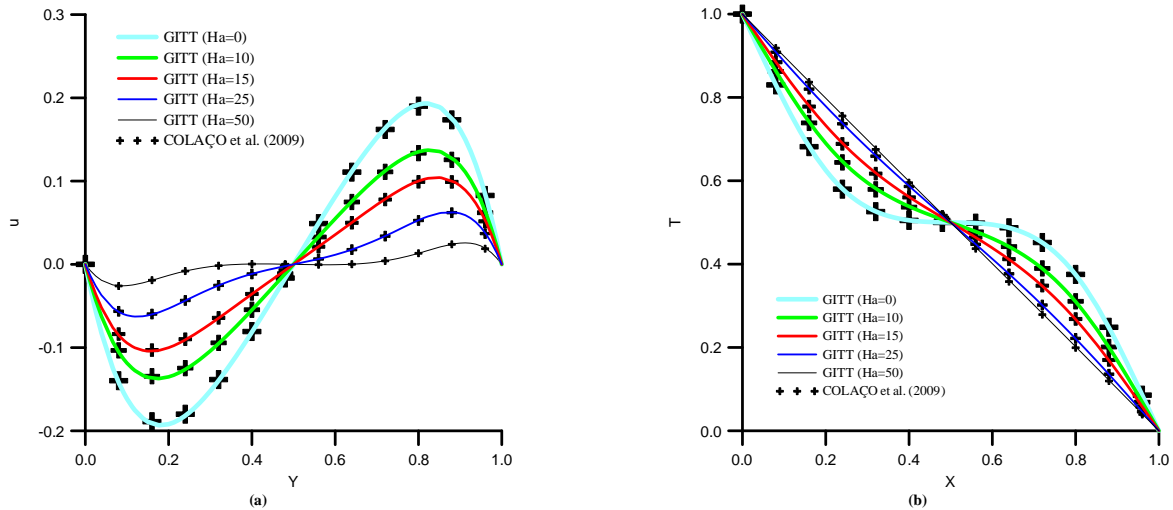
Figure 6. Comparison of the velocity and temperature fields for Gr = 10^4 at steady state: (a) velocity component u along the vertical coordinate at the cavity position x = 1/2; (b) temperature profile along the horizontal coordinate at the cavity position y =1/2.
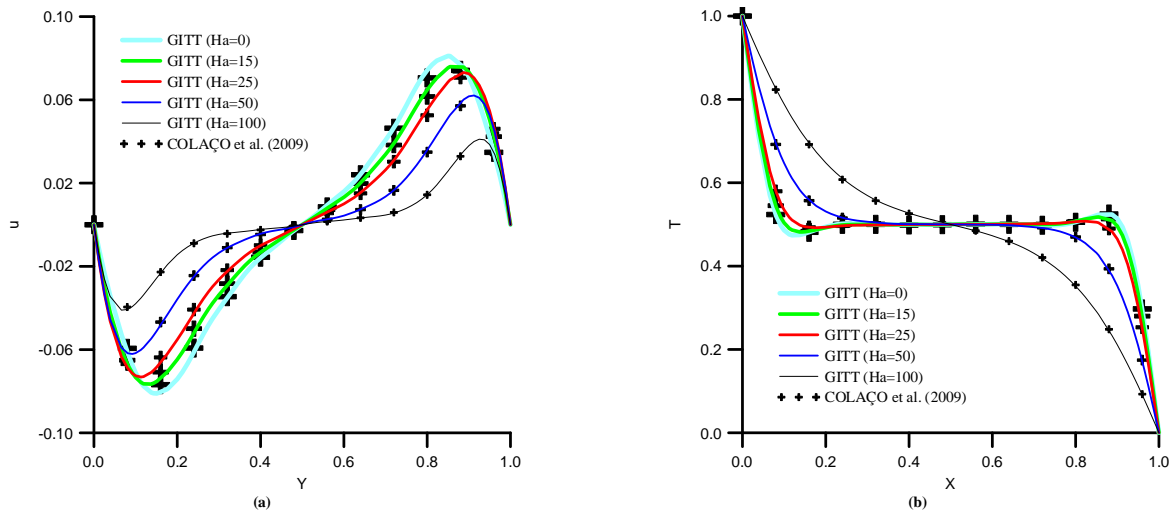
Figure 7. Comparison of the velocity and temperature fields for Gr = 10^6 at steady state: (a) velocity component u along the vertical coordinate at the cavity position x = 1/2; (b) temperature profile along the horizontal coordinate at the cavity position y =1/2.

5. CONCLUSIONS

The present study extends the application of the Generalized Integral Transform Technique (GITT) to a natural convection problem involving two-dimensional MHD flow problem in square cavities with constant magnetic field. The hybrid technique proved to be an effective tool in obtaining accurate results for situations of high nonlinearity and coupling, allowing for a physical analysis for typical values of the governing dimensionless numbers, Grashof and Hartmann numbers. The results are shown to be in excellent agreement with those available in the literature, demonstrating the consistency of the GITT approach in handling such class of problems.

6. REFERENCES

Al-Najem, N. M., Khanafer, K. M., El-Refaee, M. M., 1998. "Numerical study of laminar natural convection in tilted enclosure with transverse magnetic field", Int. J. Numer. Methods Heat Fluid Flow 8 (6), pp. 651-672.

Barakos, G., Mitsoulis, E. and Assimacopoulos, D., 1994. "Natural convection flow in a square cavity revisited: laminar and turbulent models with wall functions", Int. J. Numer. Methods Fluids, Vol. 18, pp. 695-719.

Colaço, M. J., Dulikravich, G. S. and Orlande, H. R. B., 2009 . "Magnetohydrodynamic using radial basis functions", Int. J. Heat Mass Transfer, Vol. 52, pp. 5932-5939.

Cotta, R. M. and Mikhailov, M. D., 1997, "Heat Conduction – Lumped Analysis, Integral Transforms, Symbolic Computation", Wiley-Interscience, New York,.

Cotta, R. M., 1993. "Integral Transforms in Computational Heat and Fluid Flow", CRC Press, Boca Raton, FL,.

De Vahl Davis, G., 1983. "Natural convection of air in a square cavity: a bench mark numerical solution", Int. J. for Numer. Methods in Fluids, Vol. 3, pp. 249-64.

Garandet, J. P., Alboussiere, T. and Moreau, R., 1992. "Buoyancy driven convection in a rectangular enclosure with a transverse magnetic Field", Int. J. Heat Mass Transfer, Vol. 35 (4), pp. 741-748.

Gray, D. D. and Giorgini, A., 1976. "The validity of the boussinesq approximation for liquids and gases", Int. J. Heat Mass Transfer, Vol. 19, pp. 545-551.

IMSL Library, 1991, "MATH/LIB", Houston, TX.

Leal, M. A., 1996, "Natural Convection in a Square Cavity for Steady-State and Transient Formulations: - The Integral Transform Method", D. Sc. Thesis, COPPE/UFRJ.

Leal, M. A., 1998. "Natural convection in enclosures". Cotta, R. M. (Ed.), "The Integral Transform Method in Thermal and Fluids Science and Engineering", Begell House Inc, New York, pp. 375-395.

Leal, M. A., Machado, H. A. and Cotta, R. M., 2000. "Integral Transform solutions of transient natural convection in enclosures with variable fluid properties", Vol. 43, pp. 3977-3990.

Leal, M. A., Pérez Guerrero, J. S. and Cotta, R. M., 1999. "Natural convection inside two-dimensional cavities the integral transform method", Comm. Num. Meth. Eng 15, pp.113-125.

Mikhailov, M. D. and Cotta, R. M., 1996. "Ordering rules for double and triple eigenseries in the solution of multidimensional heat and fluid flow problems", Int. Comm. Heat and Mass Transfer 23, pp. 299-303.

Oreper, G. M. and Szekely, J., 1983. "The effect of an external imposed magnetic field on buoyancy driven flow in a rectangular cavity", J. Crystal Growth, Vol. 64, pp. 505-515.

Pérez Guerrero, J. S., 1995, "Integral transformation of the Navier-Stokes equations for laminar flow in channels of arbitrary two-dimensional geometry". D. Sc. Thesis, PEM/COPPE/UFRJ, Brazil,

Ramaswany, B., Jue, T. C. and Akin, J. E., 1992, "Finite element analysis of oscillatory flow heat transfer inside a square cavity", AIAA Journal, Vol. 30 (2), pp. 412-422.

Sai, B. V. K. S., Seethamaru, K. N. and Narayana, P. A. A., 1994. "Solution of transient laminar natural convection in square cavity by an explicit finite element scheme", Numerical Heat Transfer, Vol. 25 (A), pp. 593-609.

Wolfram, S., 2005, "MATHEMATICA – a system for doing mathematics by computer, in: The Advanced Book Program", Addison Wesley, Reading, MA,.

7. RESPONSIBILITY NOTICE

The authors are the only responsible for the printed material included is this paper.